Cathepsin A-related arteriopathy with strokes and leukoencephalopathy (CARASAL)

Bugiani, M.; Kevelam, S.H.; Bakels, H.S.; Waisfisz, Q.; Ceuterick-de Groote, C.; Niessen, H.W.M.; ... ; Knaap, M.S. van der

Cathepsin A–related arteriopathy with strokes and leukoencephalopathy (CARASAL)

Marianna Bugiani, MD, PhD*
Sietske H. Kevelam, MD*
Hannah S. Bakels, MSc
Quinten Waisfisz, PhD
Chantal Ceuterick-de Groote, PhD
Hans W.M. Niessen, MD, PhD
Truus E.M. Abbink, PhD‡
Saskia A.M.J. Lesnik Oberstein, MD, PhD‡
Marjo S. van der Knaap, MD, PhD

Correspondence to Dr. van der Knaap: ms.vanderknaap@vumc.nl

ABSTRACT

Objective: To characterize the clinical and MRI features of 2 families with adult-onset dominant leukoencephalopathy and strokes and identify the underlying genetic cause.

Methods: We applied MRI pattern recognition, whole-exome sequencing, and neuropathology.

Results: Based on brain imaging, 13 family members of 40 years or older from 2 families were diagnosed with the disease; in 11 family members of the same age, MRI was normal. In the affected family members, MRI showed a leukoencephalopathy that was disproportionately severe compared to the clinical disease. The clinical picture was dominated by ischemic and hemorrhagic strokes, slow and late cognitive deterioration, and therapy-resistant hypertension. With whole-exome sequencing, we identified one variant shared by both families and segregating with the disease: c.973C>T in *CTSA*. Haplotype analysis revealed a shared 1,145-kb interval encompassing the *CTSA* variant on chromosome 20q13.12, suggesting a common ancestor. Brain autopsy of 3 patients showed a leukoencephalopathy that was disproportionately extensive compared to the vascular abnormalities. *CTSA* encodes cathepsin A. Recessive *CTSA* mutations cause galactosialidosis. One of the numerous cathepsin A functions is to degrade endothelin-1. In the patients, striking endothelin-1 immunoreactivity was found in white matter astrocytes, correlating with increased numbers of premyelinating oligodendrocyte progenitors. This finding supports a role for endothelin-1 in the leukoencephalopathy through inhibition of oligodendrocyte progenitor maturation.

Conclusions: CARASAL (cathepsin A–related arteriopathy with strokes and leukoencephalopathy) is a novel hereditary adult-onset cerebral small vessel disease. It is of interest that, next to the cerebral vascular abnormalities, endothelin-1 may have a role in the pathogenesis of the extensive leukoencephalopathy. ***Neurology*® 2016;87:1777–1786**

GLOSSARY

CAA = cerebral amyloid angiopathy; **CADASIL** = cerebral autosomal dominant arteriopathy with subcortical infarcts and leukoencephalopathy; **CARASAL** = cathepsin A–related arteriopathy with strokes and leukoencephalopathy; **CARASIL** = cerebral autosomal recessive arteriopathy with subcortical infarcts and leukoencephalopathy; **CathA** = cathepsin A; **EM** = electron microscopy; **ET-1** = endothelin-1; **GFAP** = glial fibrillary acidic protein; **MBP** = myelin basic protein; **OPC** = oligodendrocyte progenitor cell; **PAS** = periodic acid–Schiff; **PDGFRα** = platelet-derived growth factor α receptor; **SDS-PAGE** = sodium dodecyl sulfate–polyacrylamide gel electrophoresis; **SVD** = small vessel disease; **WES** = whole-exome sequencing.

Vascular brain white matter abnormalities are common among adults, especially the elderly. Most are attributed to vascular risk factors such as age, hypertension, hypercholesterolemia, diabetes mellitus, and smoking.[1,2] Only a few patients are diagnosed with hereditary small vessel disease (SVD), including cerebral autosomal dominant arteriopathy with subcortical infarcts and leukoencephalopathy (CADASIL),[3] cerebral autosomal recessive arteriopathy with subcortical infarcts and leukoencephalopathy (CARASIL),[4,5] heterozygous *HTRA1* mutations,[6] defects in collagen IVA1 and IVA2,[7,8] *TREX1*-related disorders,[9] and hereditary cerebral amyloid

Editorial, page 1752

Supplemental data at Neurology.org

*These authors contributed equally to this work.

‡These authors contributed equally to this work.

From the Departments of Child Neurology (M.B., S.H.K., H.S.B., T.E.M.A., M.S.v.d.K.) and Pathology (M.B., H.W.M.N.), Neuroscience Campus Amsterdam, VU University Medical Center, Amsterdam; Department of Clinical Genetics (Q.W.), VU University Medical Center, Amsterdam, the Netherlands; Laboratory for Ultrastructural Neuropathology (C.C.-d.G.), Institute Born-Bunge and University of Antwerp, Belgium; Department of Clinical genetics (S.A.M.J.L.O.), Leiden University Medical Center, Leiden; and Department of Functional Genomics (M.S.v.d.K.), Center for Neurogenomics and Cognitive Research, VU University, Amsterdam, the Netherlands.

Go to Neurology.org for full disclosures. Funding information and disclosures deemed relevant by the authors, if any, are provided at the end of the article.

angiopathy (CAA).[10] For several familial SVDs, the genetic cause remains unknown.[11–14] We report 2 families with adult-onset dominant leukoencephalopathy and ischemic and hemorrhagic strokes, characterized by distinct MRI and pathology findings. Whole-exome sequencing (WES) revealed one variant segregating with the disease.

METHODS

Patients. We identified a Caucasian Dutch family (F1) with adult-onset leukoencephalopathy by similar brain MRI findings. Family members younger than 40 years without MRI or with normal MRI were considered to have unknown status and were excluded; 22 family members of 40 years or older were included. Based on MRI, 11 were diagnosed with vascular leukoencephalopathy and 11 were unaffected. The pedigree indicated autosomal dominant inheritance (figure e-1 at Neurology.org). We identified 2 patients from another presumably unrelated, Caucasian Dutch family (F2). The index patient (F2-2) had similar MRI findings to F1 patients. Her father (F2-1) had cerebral white matter hypodensities on CT. No other F2 members were available.

Standard protocol approvals, registrations, and patient consents. We received approval of the ethical standards committee for gene identification studies on patients with unclassified leukoencephalopathies, and written informed consent was obtained from all included family members.

Whole-exome sequencing. In F1, we performed WES in 2 patients (F1-IV3 and F1-IV13) and one unaffected individual (F1-IV5) using the SeqCap EZ Human Exome Library v2.0 kit (Nimblegen; Roche, Madison, WI) (IV5) and SeqCap EZ Human Exome Library v3.0 kit (Nimblegen) (IV3 and IV13) on a HiSeq2000 (Illumina, San Diego, CA). Data analysis was performed as previously described.[15] Detailed information on WES methods and filtering is provided in the e-Methods and in table 1.

Molecular screening of candidate genes and variants. We performed Sanger sequencing to confirm the 2 candidate variants in *CTSA* (NM_000308.2) and *TTPAL* (NM_024331.3) identified with WES and their segregation with the disease. All included individuals of F1 were tested for the presence of the c.973C>T *CTSA* variant and c.544G>A *TTPAL* variant. All exons and exon-intron boundaries of *CTSA* and *TTPAL* were sequenced in patient F2-2, followed by confirmation of the c.973C>T *CTSA* variant in her father.

Two-point linkage analyses. We performed 2-point linkage analysis for the candidate variant using the easyLINKAGE software package running SuperLink v1.6 in F1 (details in e-Methods).

Microsatellite marker analysis. We performed haplotype analysis for F1 and F2-2 using microsatellite markers spanning the region of interest on chromosome 20q13.12 (details in e-Methods).

Neuropathology, immunohistochemical analysis, electron microscopy, and Western blots. We obtained brain tissue from patients F1-III1, F1-III2, and F1-IV8 at autopsy. Patient F1-IV8 also underwent body autopsy. For control studies, we obtained brain samples from 2 individuals (ages 27 and 57 years) without neurologic complaints and confounding neuropathology, 2 individuals (78 and 79 years) with hypertension-related sporadic SVD, one individual with sporadic capillary CAA (75 years), and one individual with CADASIL (69 years).

We stained sections for Hematoxylin & Eosin, periodic acid–Schiff (PAS), Klüver-PAS, Gomori trichrome, and elastic van Gieson. For immunostaining, we used antibodies against cathepsin A (CathA), glial fibrillary acidic protein (GFAP), endothelin-1 (ET-1), β-amyloid, phosphorylated tau, oligodendrocyte transcription factor 2, and platelet-derived growth factor α receptor (PDGFRα).[16] We quantified the degree of vessel wall changes by calculating the sclerotic index, which is the ratio of lumen diameter/external diameter, representing the degree of lumen narrowing. We performed electron microscopy (EM) on white matter from 3 patients. We counted the percentage of oligodendrocyte transcription factor 2/PDGFRα double-positive premyelinating oligodendrocyte progenitor cells (OPCs) in white matter of patients, controls with sporadic SVD, and nonneurologic controls. We compared results with 1-way analysis of variance with subsequent Bonferroni multiple comparisons test. We performed Western blotting and sodium dodecyl sulfate–polyacrylamide gel electrophoresis (SDS-PAGE) of CathA and myelin basic protein (MBP) in white matter of patients, controls with sporadic SVD, and nonneurologic controls. Details of immunohistochemistry, EM, Western blotting, and SDS-PAGE are provided in the e-Methods.

CathA activity assessment. We measured carboxypeptidase, β-galactosidase, and neuraminidase-1 activity in leukocytes in patients F1-IV3 and F1-IV13 using standard clinical testing.

RESULTS

MRI findings. MRI abnormalities were similar for F1 and F2 patients (figure 1; details in table e-1). The MRI pattern was characterized by signal changes in the frontoparietal periventricular and deep white matter that were patchy in younger patients (figure 1, A–H) and became diffuse with increasing age (figure 1, I–L). The temporal white matter was relatively spared and the temporal poles were not affected. Small multifocal areas of signal abnormality were seen in basal nuclei, thalami, internal and external capsules, and brainstem (especially pons and around midbrain red nuclei), which were more confluent in older patients (figure 1, A–C, E–G, and I–K). Seven patients had infarcts in basal nuclei, brainstem, cerebellum, or cerebral hemispheres (figure 1, M and N). Some infarcts were acute with restricted diffusion (figure 1O). Three patients had microbleeds and one had a small hemorrhage (figure 1P). Infarcts and microbleeds were more prominent in older patients. Medial temporal lobe atrophy score was 0 (normal) for all except the oldest patient, F1-III2, who had a score of 1. All unaffected individuals had a normal brain MRI.

Clinical and laboratory findings. Detailed information is provided in table e-2. First symptoms, ranging from headaches, migraines, and gait problems, to strokes, were noted in the third to fifth decade. Most patients had signs of vascular disease with hypertension requiring multiple drugs, strokes, and TIAs. Many complained of mild cognitive impairment. None of the unaffected family members had similar complaints.

Table 1 Whole-exome sequencing variant filtering and candidate gene identification

Total identified variants in sequenced family members	IV3 patient	IV5 healthy sib	IV13 patient
Total variants[a]	22,274	19,135	21,666
Variant filtering	**IV3**	**IV5**	**IV13**
Excluding segmental duplications and variants located on X chromosome	18,826	16,296	18,268
Frequency filter[b]: Excluding variants with MAF >0.001 (0.1%) in 1000 Genomes database, EVS database, and dbSNP137 database	989	871	944
Inheritance: Excluding variants without autosomal dominant inheritance pattern[c]		63	
In-house control: Excluding variants present in our in-house control database[d]		3	
Pathogenicity: Excluding synonymous variants not adjacent to splice site		2 (see below)	

Identified candidate variants

Gene	c.DNA[e]	Protein	Effect	Chromosome	Conservation	Pathogenicity[f]	ExAC[g] database	Confirmed[h]
CTSA	c.922C>T	Arg308Cys	Missense	20q13	Up to *C elegans*	Damaging	Not present	Yes
TTPAL	c.544G>A	Gly182Arg	Missense	20q13	Up to fruit fly	Damaging	Not present	Yes

Abbreviations: *C elegans* = *Caenorhabditis elegans*; EVS = Exome Variant Server; ExAC = Exome Aggregation Consortium; MAF = minor allele frequency; sib = sibling.
Nomenclature according to Human Genome Variation Society (http://www.hgvs.org/mutnomen).
[a] Including both detected insertions and deletions and single nucleotide variants.
[b] Three public variant databases were used: (1) dbSNP137 (http://www.ncbi.nlm.nih.gov/projects/SNP), (2) 1000 Genomes Project (release of February 2012), (3) EVS, National Heart, Lung, and Blood Institute GO Exome Sequencing Project (ESP5400 release) (http://evs.gs.washington.edu/EVS/).
[c] Autosomal dominant inheritance was defined as a heterozygous variant (≥32% and ≤69% of the reads harbored the alternative allele) present in both affected family members IV3 and IV13 and absent in a heterozygous or homozygous state in the unaffected individual IV5. Variants with a minimal coverage of 5 reads in both affected individuals were considered.
[d] The in-house control database contained 21 exomes.
[e] *CTSA* reference sequence: NM_000308.2; *TTPAL* reference sequence: NM_024331.3.
[f] Pathogenicity prediction of variants was calculated with SIFT, PolyPhen-2, and MutationTaster.
[g] ExAC, Cambridge, MA (URL: http://exac.broadinstitute.org) (accessed March 2016).
[h] Investigated with Sanger sequencing.

Only 2 had hypertension, which was controlled with a single drug. Smoking and alcohol consumption were similar between patients and unaffected individuals. Patients also had more nonneurologic complaints than unaffected family members, including dry mouth with difficulty swallowing, dry eyes, and muscle cramps. Physical examination of patients showed at most mild neurologic abnormalities. Laboratory findings, including β-galactosidase, neuraminidase-1, and carboxypeptidase activity in leukocytes were unremarkable. Sanger sequencing of all *NOTCH3* exons and exon-intron boundaries, except the noncoding exon 1, did not identify pathogenic variants in 3 F1 patients and the F2-2 patient. *COL4A1* and *COL4A2* were sequenced in F2-2 and showed no pathogenic variants. In F1 patients IV3 and IV13, additional Sanger sequencing of exon 1, which was not sufficiently covered by WES, revealed no pathogenic *HTRA1* variants.

Genetic analysis. WES in 3 family members of F1, 2 affected and 1 unaffected, revealed 2 heterozygous candidate variants in 2 genes: c.973C>T, p.(Arg325Cys) in *CTSA* and c.544G>A, p.(Gly182Arg) in *TTPAL*, both located on chromosome 20q13.12 (table 1). *CTSA* encodes CathA; *TTPAL* encodes tocopherol (alpha) transfer protein-like (TTPAL). Both unknown variants segregated with the disease in F1 (figure e-1). Only the same heterozygous *CTSA* variant was found in patient F2-2 and her father, leaving *CTSA* as the only shared candidate gene. The c.973C>T *CTSA* variant (NP_000299, p.[Arg325Cys]) is absent from public databases, including dbSNP, 1000 Genomes Project, Exome variant server and genome of the Netherlands (GoNL[17]) database, and the Exome Aggregation Consortium, Cambridge, MA (URL: http://exac.broadinstitute.org). In silico programs predict the mutation to be damaging.

Two-point linkage analysis for the *CTSA* variant in F1 showed a maximal logarithm of odds score of 5.4953 at theta 0 for the variant.

Haplotype analysis around the *CTSA* locus. Using 13 consecutive microsatellite markers, we identified among F1 patients a shared haplotype of 8 consecutive

Figure 1 MRI findings

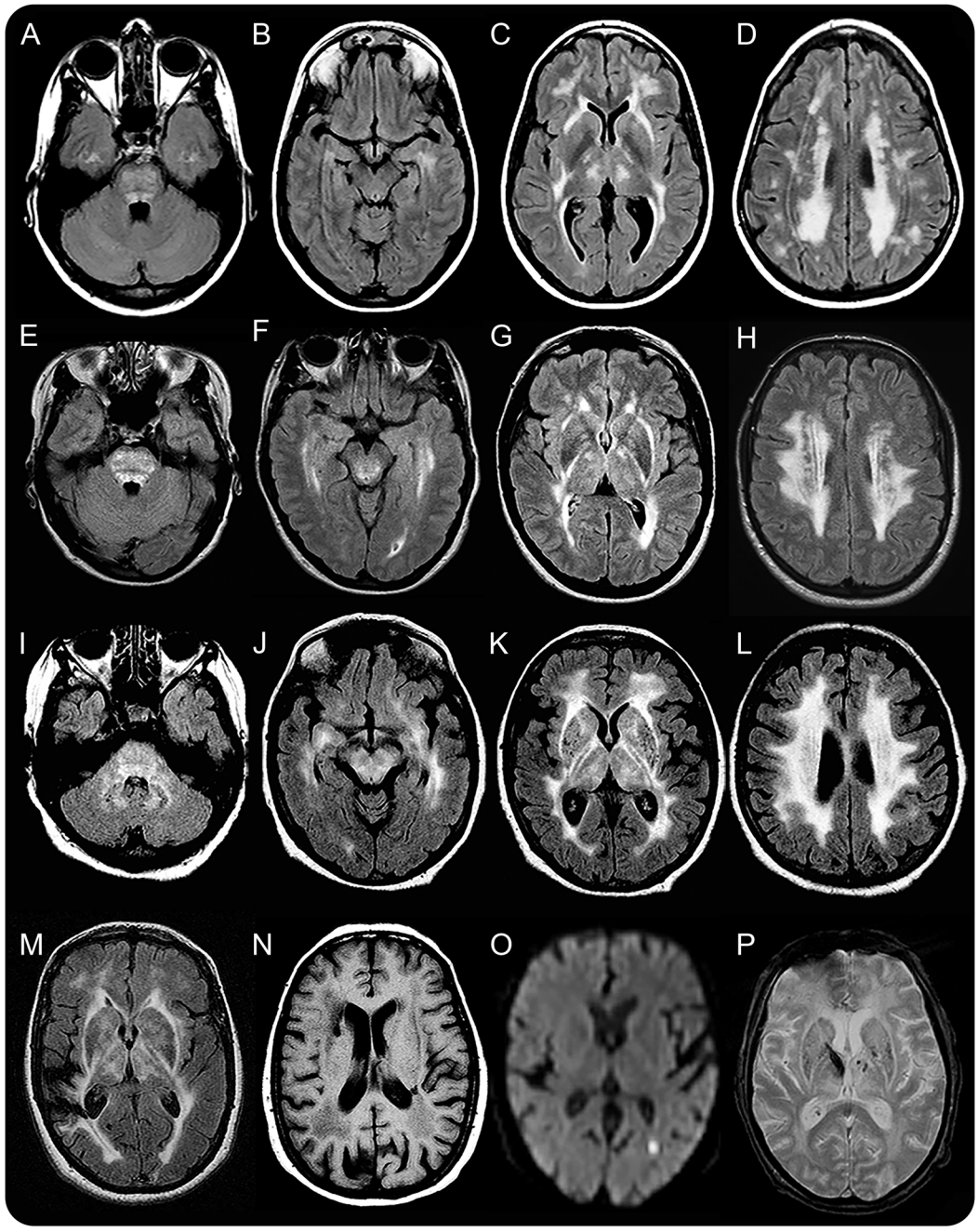

Axial fluid-attenuated inversion recovery images of patient F2-2 (39 years) (A–D), patient F1-IV6 (46 years) (E–H), patient F1-III1 (67 years) (I–L), and patient F1-III5 (69 years) (M); T1-weighted image of patient F1-III4 (73 years) (N); DWI of patient F1-IV8 (53 years) (O); gradient echo image of patient F1-III2 (P). MRIs show the multifocal to confluent white matter abnormalities located predominantly in the frontoparietal deep and periventricular white matter (B–D, F–H, J–L), the basal nuclei, thalamus, and the internal and external capsule (C, G, K). The pons shows multifocal T2-hyperintensities, even at an early age (A and E). The white matter abnormalities are more extensive in the elder patients (compare figures A–H and I–L). Patient F1-III5 had a large infarct located in the right temporoparietal region (M). Small cystic infarcts are seen in the periventricular white matter (N). Some infarcts are acute, as indicated by a high signal on DWI (O) and a low signal on apparent diffusion coefficient maps (not shown). Microbleeds and a small hemorrhage are seen in the basal nuclei and thalamus (P). DWI = diffusion-weighted image.

markers flanked by markers D20S46 and D20S891 (physical genomic location Hg19 chr20: 41334729–45929596) (not shown), which was not shared by any of the unaffected F1 individuals. Marker analysis for patient F2-2 showed that she shared identical alleles for 2 adjacent markers close to *CTSA* (see table e-3), suggestive of common ancestry of the allele. The smallest putative shared region was 1,145 kilobases (kb), flanked by microsatellite markers D20S481 and D20S836 (Hg19 chr20: 43768281–44940373). This

interval contains 58 genes (24 with OMIM annotation), including *CTSA* but not *TTPAL*.

Neuropathologic findings. Gross examination (figure 2A) showed mild cerebral white matter atrophy and scattered small infarcts in subcortical and deep cerebral white matter, basal nuclei, thalami, brainstem, and cerebellum.

Microscopy revealed an extensive leukoencephalopathy with myelin pallor, relatively preserved axons,

Figure 2 Neuropathologic findings

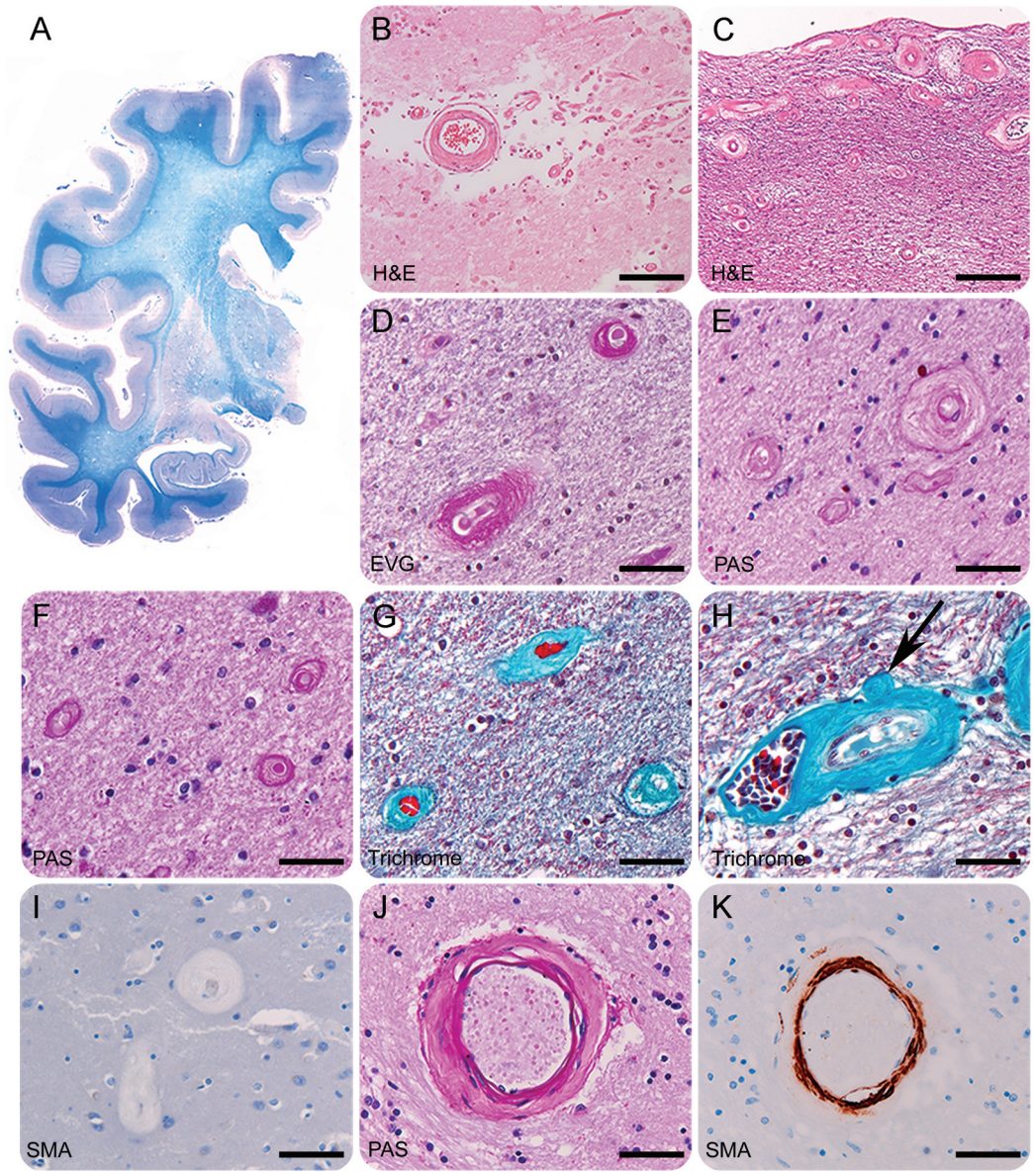

Whole mount of the right cerebral hemisphere of patient F1-III2 at the level of the anterior hippocampus stained with the Klüver stain for myelin (blue) and PAS (purple) shows diffuse white matter pallor extending to the internal and external capsules and, in places, the U fibers. The lateral ventricle is slightly enlarged, indicating mild white matter atrophy. The cortex and hippocampus are not involved (A). Ischemic lesions in the white matter (B, patient F1-III1) appear as areas of enlargement, rarefaction, and loosening of the perivascular tissue with presence of foamy macrophages (H&E). The small arterioles along the wall of the lateral ventricle show asymmetric fibrous thickening of the vessel wall with luminar stenosis (C, H&E, patient F1-III2). Similar changes are also visible in the subcortical (D, EVG, patient F1-IV8) and deep hemispheric white matter (E, PAS, patient F1-III2) and in white matter bundles in the striatum (F, PAS, patient F1-III1) and pons (G, Gomori trichrome, patient IV8). Note the loss of vascular elastic fibers (D, EVG), the absence of PAS-positive material (E and F, PAS), and the asymmetric fibrous thickening of the small arteriolar walls (G, Gomori trichrome). The vasa vasorum of the larger arterioles (arrow) may be totally occluded (H, Gomori trichrome, patient F1-III2). Stain against SMA (I, patient F1-IV8) shows complete degeneration of vascular smooth muscle cells. In sporadic small vessel disease (J and K), small arteries show symmetric thickening of the vessel wall with concentric accumulation of extracellular matrix components (J, PAS) and less severe degeneration of vascular smooth muscle cells (K, SMA). Bars: (B–C) 200 μm; (D–K) 100 μm. EVG = elastic van Gieson; H&E = hematoxylin & eosin; PAS = periodic acid–Schiff; SMA = smooth muscle actin.

some without myelin, astrogliosis, and preserved oligodendrocytic density. Lacunar changes, consisting of perivascular tissue rarefaction with macrophages, focal oligodendrocyte and axonal loss, and astrogliosis, were abundant in patients F1-III1 and F1-III2 (figure 2B) but few in F1-IV8. In all patients and in the controls with sporadic SVD, arterioles showed diffuse angiosclerosis. There was no accumulation of basophilic, PAS-positive, or congophilic material. Labeling for β-amyloid was negative (not shown). Of note, in patients with *CTSA* mutation but not in the neurologic and nonneurologic controls, we detected unusual changes involving distal arteriolar branches, consisting of vessel wall fibrous thickening, which was remarkably asymmetric, and loss of smooth muscle cells with near-total occlusion of the lumen. These changes were present throughout the cerebral white matter, basal nuclei, and subependymal regions, and also involved vasa vasorum (figure 2, C–I). Perivascular dystrophic calcifications and inflammatory cells were negligible. These microvascular changes were different from what was found in the neurologic controls (figure 2, J and K). Calculation of the sclerotic index revealed more severe lumen narrowing in our patients (mean 0.55) than in sporadic SVD (mean 0.33) and normal controls (mean 0.27). Patients F1-III1 and F1-III2 also showed mild Alzheimer disease–related changes scored as A1B1C0.[18]

EM of white matter blood vessels confirmed absence of granular osmiophilic material close to smooth muscle cells and amyloid. Terminal arterioles showed asymmetrically enlarged tunica adventitia with accumulation of elastic, normal-appearing collagen fibrils and, in some vessels, focal thickening of the basal lamina (not shown). In the noninfarcted white matter, EM confirmed the presence of axons without myelin (not shown).

In the noninfarcted cerebral white matter, OPC numbers were higher in patients with *CTSA* mutation than in sporadic SVD ($p < 0.05$), and in both compared to nonneurologic controls ($p < 0.01$ and $p < 0.001$, respectively) (figure 3H). The amounts of the myelin protein MBP were lower in patients than in controls with sporadic SVD (figure 3I).

Body autopsy of patient F1-V8 revealed atherosclerosis in the aorta and larger arteries without ulcerated plaques or signs of major vascular disease, and diffuse glomerulosclerosis in the kidneys.

CathA and ET-1 protein immunoreactivity in the brain. Nonneurologic controls showed delicate cytoplasmic CathA immunoreactivity in neurons and astrocytes at the glia limitans and around blood vessels in gray and white matter. At these sites, increased CathA labeling was observed in patients and, to a lesser degree, all neurologic controls (data not shown). In the white matter of patients and neurologic controls, intense cytoplasmic CathA immunoreactivity was seen in reactive astrocytes. However, in neurologic controls, CathA-positive astrocytes were only present around infarcts, whereas in patients with *CTSA* mutation, strongly CathA-expressing astrocytes were present throughout the white matter (figure 3, A–F).

We investigated CathA accumulation in reducing and nonreducing SDS-PAGE Western blotting to assess whether the additional cysteine residue causes aberrant disulfide bridge formation and consequent protein misfolding.[19,20] Abnormal foldings would only be detected under nonreducing conditions that leave disulfide bridges intact. We did not detect these in patients or controls. However, under all conditions, the CathA 54-kDa precursor protein was increased in patients with *CTSA* mutation compared to neurologic and nonneurologic controls. Of note, the amounts of CathA precursor protein were similar in sporadic SVD and the nonneurologic control. The amounts of the mature 20-kDa CathA product were not significantly changed in patients with *CTSA* mutation (figure 3G).

ET-1 is a peptide degraded by CathA that has roles in vasoconstriction and OPC maturation.[21,22] We found ET-1–positive reactive astrocytes around infarcts in patients and all neurologic controls. In noninfarcted white matter areas, however, astrocytic ET-1 immunolabeling was strikingly higher in patients than in neurologic controls (figure 3, J and K). Astrocytes in nonneurologic controls were ET-1 negative (figure 3L).

DISCUSSION We report 2 families with adult-onset dominant "cathepsin A–related arteriopathy with strokes and leukoencephalopathy" (CARASAL), presenting with therapy-resistant hypertension, ischemic and hemorrhagic strokes, and late cognitive deterioration. Complaints of dry eyes and mouth, and muscle cramps are consistent additional features in F1, but not F2. MRI initially shows multifocal signal changes in the cerebral white matter and basal nuclei, thalami, and brainstem, a pattern suggestive of SVD.[23] Over time, the leukoencephalopathy becomes virtually diffuse. As in other SVDs, the leukoencephalopathy on MRI precedes the onset of strokes and is disproportionate to the clinical severity.[24]

The clinical, MRI, and especially pathology phenotypes in our families do not suggest a known autosomal dominant vasculopathy. EM showed no granular osmiophilic material, basal lamina fragmentation or multilamination, or amyloid deposition in blood vessels, as seen in CADASIL, defects of collagen IVA1 and IVA2, *TREX1*-related disease, and CAA, respectively.[3,7,8,25–27] *NOTCH3* sequencing was unrevealing and WES showed no known or possible pathogenic variants in *COL4A1*, *COL4A2*, *TREX1*, and CAA-related genes,

Figure 3 Increased CathA and ET-1 expression correlates with increased OPC numbers and lack of myelin

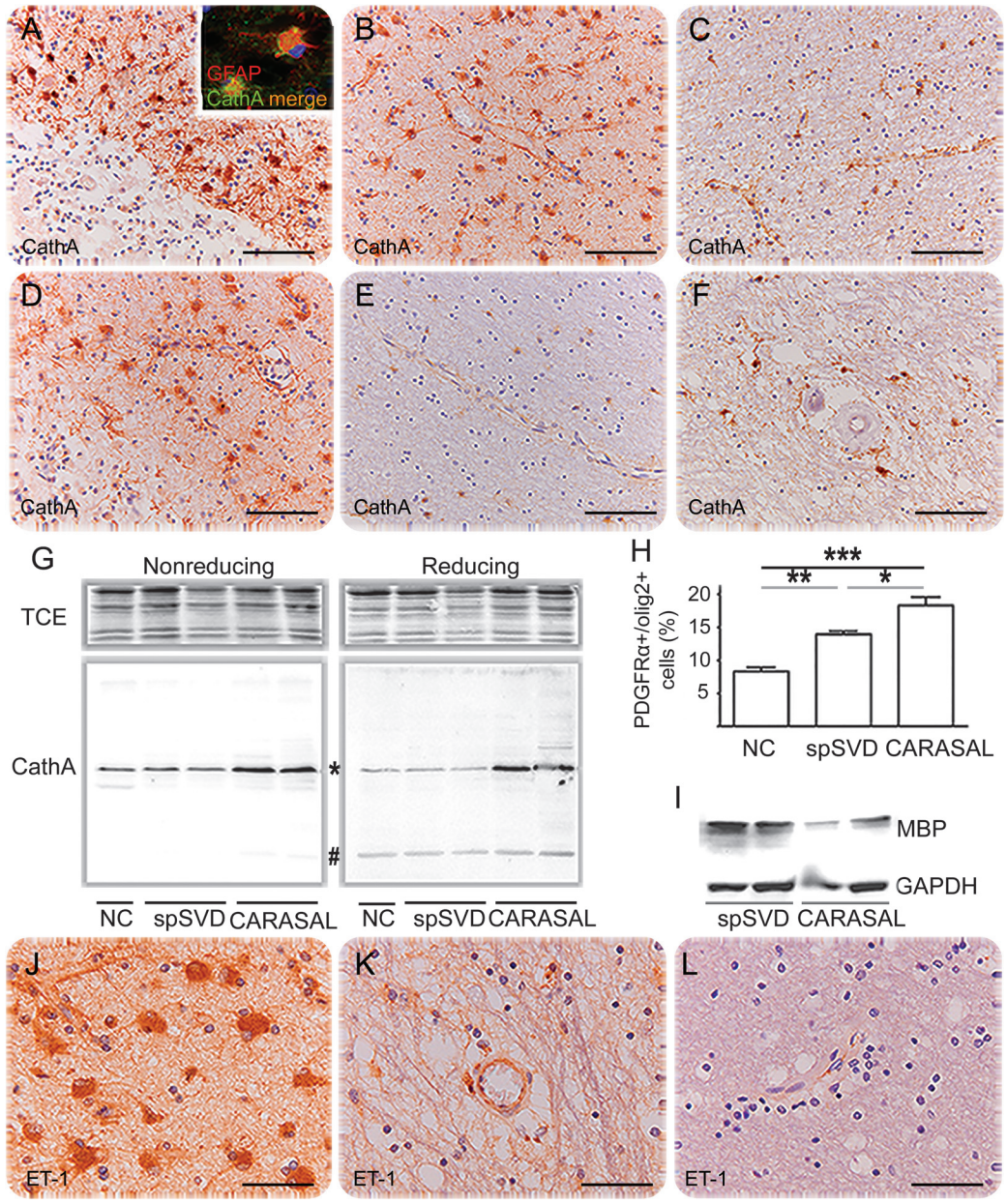

Patients (A and B) show increased CathA immunoreactivity compared to controls with capillary cerebral amyloid angiopathy (C), sporadic SVD (D and E), and CADASIL (F) in astrocytes both surrounding infarcts (A and D) and in white matter areas distant from infarcted areas (B, C, E, and F). The CathA-positive cells have the morphology of astrocytes and express the astrocyte-specific marker GFAP (inset in A, GFAP in red and CathA in green). Western blotting of white matter lysates in nonreducing (left panel) and reducing sodium dodecyl sulfate–polyacrylamide gel electrophoresis (right panel) show increased amounts of the CathA precursor protein (*, 54 kDa) in patients F1-III1 and F1-III2 compared to a nonneurological control and 2 controls with sporadic SVD. The amounts of mature CathA protein (#, 20 kDa) are not evidently changed. Note that the additional faint bands of different molecular weight present on both blots are not specific for the patients (G). In white matter areas devoid of lacunar infarcts, the patients' white matter astrocytes (J, patient F1-III2) are more intensely ET-1 immunoreactive than those of controls with sporadic SVD (K). White matter astrocytes of a nonneurologic control are ET-1 negative (L). The percentage of PDGFRα-positive premyelinating OPCs is significantly higher in the white matter of the patients than of controls with sporadic SVD and the nonneurologic control (*$p < 0.05$, **$p < 0.01$, ***$p < 0.001$; H). Western blotting of white matter lysates shows lower amounts of MBP (upper panel) in the patients than in controls with sporadic SVD. The lower panel confirms equal protein loading (GAPDH) (I). Bars: (A–F) 100 μm; (J–L): 50 μm. CADASIL = cerebral autosomal dominant arteriopathy with subcortical infarcts and leukoencephalopathy; CARASAL = cathepsin A–related arteriopathy with strokes and leukoencephalopathy; CathA = cathepsin A; ET-1 = endothelin-1; GFAP = glial fibrillary acidic protein; MBP = myelin basic protein; NC = nonneurologic control; olig2 = oligodendrocyte transcription factor 2; OPC = oligodendrocyte progenitor cell; PDGFRα = platelet-derived growth factor α receptor; spSVD = controls with sporadic small vessel disease; SVD = small vessel disease; TCE = trichloroethanol, indicating on-blot total protein signal.

including *APP*, *CST3*, *TTR*, *GSN*, *BRI2*, and *PRPN*. No pathogenic *HTRA1* variants were found in WES and Sanger sequencing of exon 1. The unusual pathology of the terminal arterioles observed in our patients was not present in the investigated patients with CADASIL, CAA, and sporadic SVD.

The 2 families were identified independently on the basis of MRI findings. In both, the same *CTSA* variant segregated with the disease. Haplotype analysis showed that a 1,145-kb region encompassing the *CTSA* variant is shared by the families, suggesting that the variant originates from a common ancestor. WES revealed no other dominant variants in this region, leaving *CTSA* as the only candidate gene.

Hervé et al.[14] reported a French family with autosomal dominant vascular leukoencephalopathy with an MRI pattern similar to CARASAL. Remarkably, the unusual pathologic changes of white matter small arterioles, including the vasa vasorum, were also noted.[14] The French family showed linkage with an 11.2-Mb interval on chromosome 20q13,[14] encompassing the 1,145-kb region of the *CTSA* variant,[14] a strong argument for the same disease.

CathA is synthesized as a single-chain precursor of 54 kDa that is converted into a catalytically active heterodimer consisting of 20- and 32-kDa subunits.[28,29] Mature CathA is mainly found in lysosomes, where it stabilizes a multienzyme complex with β-galactosidase and neuraminidase-1. Recessive *CTSA* mutations cause galactosialidosis due to deficiency of β-galactosidase and neuraminidase-1.[30,31] Heterozygous *CTSA* mutations have hitherto not been associated with disease.

The possible functional role of the *CTSA* mutation in CARASAL is presently unexplained. Considering the dominant inheritance, the Arg325Cys change could have a toxic effect. The extra cysteine could affect stabilization, folding, and structure of the protein because of extra disulfide bonds.[19] Nonreducing SDS-PAGE, however, did not show alternative conformations of mutant CathA. In patients with CARASAL, CathA signals in nonreducing and reducing conditions were similar, excluding the possibility of CathA isoforms being too large to enter the gel. These findings do not support misfolding of mutant CathA.

In our patients, CathA-expressing astrocytes were spread over the white matter, whereas in capillary CAA, CADASIL, and sporadic SVD, they only clustered around infarcts. Reducing SDS-PAGE confirmed increased CathA precursor protein amounts in patients with CARASAL only. Of note, CathA was not increased in controls with sporadic SVD and similar degree of vascular lesions and reactive gliosis, indicating that the observed CathA accumulation is not merely a consequence of the small vessel involvement and ischemic pathology.

Leukoencephalopathy is part of the general SVD histopathology phenotype, with loss of oligodendrocytes, myelin, and axons centered on abnormal vessels.[32] The pathomechanism of SVD-related leukoencephalopathy is complex, also involving chronic hypoperfusion and hypoxia.[32] White matter pathology in CARASAL shows paucity of myelin, astrogliosis, and increased OPC numbers extending *beyond* the ischemic pathology, also present in patient F1-IV8 who had no infarcts and few lacunae. The discrepancy between extensive white matter involvement and relatively mild vascular lesions in CARASAL suggests that additional pathomechanisms besides ischemia contribute to the leukoencephalopathy.

We investigated ET-1, a peptide with roles in vasoconstriction[21] and OPC maturation,[22] which is degraded by CathA carboxypeptidase and other proteases.[33,34] We found strikingly increased ET-1 immunoreactivity in CARASAL white matter astrocytes, also compared to other vascular leukoencephalopathies. Astrocyte-derived ET-1 may contribute to long-lasting vasoconstriction and hypoxia.[35] Transgenic mice with selective inactivation of CathA carboxypeptidase have hypertension due to reduced ET-1 degradation,[36] a feature shared by patients with CARASAL. In CARASAL, ET-1 overexpression coincides with increased numbers of premyelinating OPCs, decreased MBP amounts, and abundance of axons without myelin, features of remyelination failure. Findings in multiple sclerosis indicate that astrocyte-derived ET-1 may inhibit OPC maturation.[22] Strikingly, in multiple sclerosis, ET-1–expressing astrocytes are found only within demyelinating lesions,[22] whereas in CARASAL, they are present throughout the noninfarcted white matter. It is tempting to speculate that ET-1 accumulates in CARASAL because of the *CTSA* mutation. This would imply that CathA carboxypeptidase activity is reduced in patients' brain, although reduced activity was not found in leukocytes. In this scenario, ET-1 would contribute to the leukoencephalopathy in CARASAL and explain the extensive white matter abnormalities far beyond the vascular injury.

Arterial hypertension with cortical-subcortical infarctions has been reported in a single patient with galactosialidosis.[37] Parents of patients with galactosialidosis, who are obligatory *CTSA* mutation carriers, are not known to have increased risk of hypertension and SVD. However, since galactosialidosis is rare and hypertension and hypertension-related white matter lesions are common, such association may have easily been overlooked. Similar oversights have occurred before.[38,39] It is long known that Gaucher disease is caused by recessive mutations in *GBA1*, encoding glucocerebrosidase. Only recently it has become clear that heterozygous carriers of *GBA1* mutations have an increased risk of Parkinson disease and Lewy body dementia.[38] It is

worthwhile to investigate whether heterozygous *CTSA* mutations are associated with an increased risk of SVD in families of patients with galactosialidosis. Further studies should elucidate whether only the p.(Arg325Cys) variant in *CTSA* is associated with CARASAL or whether the risk of an SVD is also seen in other mutations.

Vascular leukoencephalopathies are common in elderly individuals. With CARASAL, a new phenotype is added to the spectrum. We suspect that the genetic origin of adult-onset vascular leukoencephalopathies is often overlooked.

AUTHOR CONTRIBUTIONS

Marianna Bugiani performed autopsies, designed, supervised, and interpreted the histopathology, immunohistochemistry, electron microscopy, and participated in drafting the manuscript. Sietske H. Kevelam interpreted the MRIs, performed neurologic examinations, collected patient data, analyzed and interpreted the exome data and microsatellite data, and participated in drafting the manuscript. Hannah S. Bakels participated in performing and analyzing the histopathology and immunohistochemistry. Quinten Waisfisz analyzed and interpreted the microsatellite data and the exome data, and participated in drafting the manuscript. Chantal Ceuterick-de Groote and Hans W.M. Niessen participated in interpreting ultrastructural data. Truus E.M. Abbink designed and interpreted Western blots and participated in interpreting the immunohistochemistry and drafting the manuscript. Saskia A.M.J. Lesnik Oberstein participated in the design of the study and in drafting the manuscript. Marjo S. van der Knaap conceptualized the study, has access to all data, takes responsibility for the data, participated in the design of the study, performed neurologic examinations, interpreted the MRIs, and participated in drafting the manuscript.

ACKNOWLEDGMENT

The authors thank Carola van Berkel for performing the DNA and microsatellite analysis and Nienke Postma for performing immunohistochemistry and Western blots (Department of Child Neurology, VU University Medical Center, Amsterdam, the Netherlands); Peter Heutink (DZNE, German Center for Neurodegenerative Diseases, Tübingen, Germany) and Marianna Bevova (ERIBA, University Medical Center Groningen, the Netherlands) for supervision with the exome analysis; Orr Shomroni (DZNE, German Center for Neurodegenerative Diseases, Göttingen, Germany) and Ingrid Bakker (Department of Clinical Genetics, VU University Medical Center, Amsterdam, the Netherlands) for technical assistance; Alex Vincent Postma (Department of Anatomy, Embryology & Physiology and Department of Clinical Genetics, Academic Medical Center, the Netherlands) for performing the 2-point linkage analysis; the Netherlands Brain Bank (Amsterdam, the Netherlands) for providing brain tissue of the patients with sporadic SVD; Annemieke Rozemuller and Jeroen Hoozemans (Department of Pathology, VU University Medical Center, Amsterdam, the Netherlands) for providing the tissue of the patient with CAA; Françoise Gray (Department of Pathology, Hôpital Lariboisière, Paris, France) for providing the tissue of the patient with CADASIL and for helpful discussion of the vascular pathology; Dirk Lefeber (Department of Laboratory Medicine, Radboud University Nijmegen Medical Center, Nijmegen, the Netherlands) for determining CathA-related enzyme activities in leukocytes and providing fibroblasts of patients with galactosialidosis; and the mortuary assistants of the VU University Medical Center, Amsterdam, the Netherlands, for their skillful assistance during the autopsies.

STUDY FUNDING

The study received financial support from the ZonMw TOP grant 91211005 and the Optimix Foundation for Scientific Research.

DISCLOSURE

M. Bugiani reports no disclosures relevant to the manuscript. S. Kevelam is supported by ZonMw TOP grant 91211005. H. Bakels, Q. Waisfisz, C. Ceuterick-de Groote, H. Niessen, T. Abbink, and S. Lesnik Oberstein report no disclosures relevant to the manuscript. M. van der Knaap is supported by ZonMw TOP grant 91211005. Go to Neurology.org for full disclosures.

Received January 13, 2016. Accepted in final form June 28, 2016.

REFERENCES

1. Sahathevan R, Brodtmann A, Donnan GA. Dementia, stroke, and vascular risk factors: a review. Int J Stroke 2012;7:61–73.
2. Roman GC, Erkinjuntti T, Wallin A, Pantoni L, Chui HC. Subcortical ischaemic vascular dementia. Lancet Neurol 2002;1:426–436.
3. Joutel A, Corpechot C, Ducros A, et al. Notch3 mutations in CADASIL, a hereditary adult-onset condition causing stroke and dementia. Nature 1996;383:707–710.
4. Hara K, Shiga A, Fukutake T, et al. Association of HTRA1 mutations and familial ischemic cerebral small-vessel disease. N Engl J Med 2009;360:1729–1739.
5. Tikka S, Baumann M, Siitonen M, et al. CADASIL and CARASIL. Brain Pathol 2014;24:525–544.
6. Verdura E, Herve D, Scharrer E, et al. Heterozygous HTRA1 mutations are associated with autosomal dominant cerebral small vessel disease. Brain 2015;138:2347–2358.
7. Gould DB, Phalan FC, van Mil SE, et al. Role of COL4A1 in small-vessel disease and hemorrhagic stroke. N Engl J Med 2006;354:1489–1496.
8. Verbeek E, Meuwissen ME, Verheijen FW, et al. COL4A2 mutation associated with familial porencephaly and small-vessel disease. Eur J Hum Genet 2012;20:844–851.
9. Richards A, van den Maagdenberg AM, Jen JC, et al. C-terminal truncations in human 3′-5′ DNA exonuclease TREX1 cause autosomal dominant retinal vasculopathy with cerebral leukodystrophy. Nat Genet 2007;39:1068–1070.
10. Revesz T, Holton JL, Lashley T, et al. Genetics and molecular pathogenesis of sporadic and hereditary cerebral amyloid angiopathies. Acta Neuropathol 2009;118:115–130.
11. Verreault S, Joutel A, Riant F, et al. A novel hereditary small vessel disease of the brain. Ann Neurol 2006;59:353–357.
12. Ding XQ, Hagel C, Ringelstein EB, et al. MRI features of pontine autosomal dominant microangiopathy and leukoencephalopathy (PADMAL). J Neuroimaging 2010;20:134–140.
13. Low WC, Junna M, Borjesson-Hanson A, et al. Hereditary multi-infarct dementia of the Swedish type is a novel disorder different from NOTCH3 causing CADASIL. Brain 2007;130:357–367.
14. Hervé D, Chabriat H, Rigal M, et al. A novel hereditary extensive vascular leukoencephalopathy mapping to chromosome 20q13. Neurology 2012;79:2283–2287.
15. Kevelam SH, Bugiani M, Salomons GS, et al. Exome sequencing reveals mutated SLC19A3 in patients with an early-infantile, lethal encephalopathy. Brain 2013;136:1534–1543.
16. Bugiani M, Boor I, van KB, et al. Defective glial maturation in vanishing white matter disease. J Neuropathol Exp Neurol 2011;70:69–82.
17. Genome of the Netherlands Consortium. Whole-genome sequence variation, population structure and demographic history of the Dutch population. Nat Genet 2014;46:818–825.
18. Montine TJ, Phelps CH, Beach TG, et al. National Institute on Aging–Alzheimer's Association guidelines for the neuropathologic assessment of Alzheimer's disease: a practical approach. Acta Neuropathol 2012;123:1–11.

19. Thornton JM. Disulphide bridges in globular proteins. J Mol Biol 1981;151:261–287.
20. Duering M, Karpinska A, Rosner S, et al. Co-aggregate formation of CADASIL-mutant NOTCH3: a single-particle analysis. Hum Mol Genet 2011;20:3256–3265.
21. Kiely DG, Cargill RI, Struthers AD, Lipworth BJ. Cardiopulmonary effects of endothelin-1 in man. Cardiovasc Res 1997;33:378–386.
22. Hammond TR, Gadea A, Dupree J, et al. Astrocyte-derived endothelin-1 inhibits remyelination through notch activation. Neuron 2014;81:588–602.
23. Wardlaw JM, Smith EE, Biessels GJ, et al. Neuroimaging standards for research into small vessel disease and its contribution to ageing and neurodegeneration. Lancet Neurol 2013;12:822–838.
24. Chabriat H, Joutel A, Dichgans M, Tournier-Lasserve E, Bousser MG. Cadasil. Lancet Neurol 2009;8:643–653.
25. van der Knaap MS, Smit LM, Barkhof F, et al. Neonatal porencephaly and adult stroke related to mutations in collagen IV A1. Ann Neurol 2006;59:504–511.
26. Plaisier E, Gribouval O, Alamowitch S, et al. COL4A1 mutations and hereditary angiopathy, nephropathy, aneurysms, and muscle cramps. N Engl J Med 2007;357:2687–2695.
27. Kolar GR, Kothari PH, Khanlou N, Jen JC, Schmidt RE, Vinters HV. Neuropathology and genetics of cerebroretinal vasculopathies. Brain Pathol 2014;24:510–518.
28. Rudenko G, Bonten E, d'Azzo A, Hol WG. Three-dimensional structure of the human 'protective protein': structure of the precursor form suggests a complex activation mechanism. Structure 1995;3:1249–1259.
29. Kolli N, Garman SC. Proteolytic activation of human cathepsin A. J Biol Chem 2014;289:11592–11600.
30. d'Azzo A, Andria G, Strisciuglio P, Galjaard H. Galactosialidosis. In: Scriver CR, Beaudet AL, Sly WS, et al., editors. The Metabolic and Molecular Bases of Inherited Disease, 8th ed. New York: McGraw-Hill; 2001:3811–3826.
31. Strisciuglio P, Parenti G, Giudice C, Lijoi S, Hoogeveen AT, d'Azzo A. The presence of a reduced amount of 32-kd "protective" protein is a distinct biochemical finding in late infantile galactosialidosis. Hum Genet 1988;80:304–306.
32. Jellinger KA. The enigma of vascular cognitive disorder and vascular dementia. Acta Neuropathol 2007;113:349–388.
33. Itoh K, Kase R, Shimmoto M, Satake A, Sakuraba H, Suzuki Y. Protective protein as an endogenous endothelin degradation enzyme in human tissues. J Biol Chem 1995; 270:515–518.
34. Pshezhetsky AV, Hinek A. Serine carboxypeptidases in regulation of vasoconstriction and elastogenesis. Trends Cardiovasc Med 2009;19:11–17.
35. Zhang WW, Badonic T, Hoog A, et al. Structural and vasoactive factors influencing intracerebral arterioles in cases of vascular dementia and other cerebrovascular disease: a review. Immunohistochemical studies on expression of collagens, basal lamina components and endothelin-1. Dementia 1994;5:153–162.
36. Seyrantepe V, Hinek A, Peng J, et al. Enzymatic activity of lysosomal carboxypeptidase (cathepsin) A is required for proper elastic fiber formation and inactivation of endothelin-1. Circulation 2008;117:1973–1981.
37. Nordborg C, Kyllerman M, Conradi N, Mansson JE. Early-infantile galactosialidosis with multiple brain infarctions: morphological, neuropathological and neurochemical findings. Acta Neuropathol 1997;93:24–33.
38. Siebert M, Sidransky E, Westbroek W. Glucocerebrosidase is shaking up the synucleinopathies. Brain 2014; 137:1304–1322.
39. Tetreault M, Gonzalez M, Dicaire MJ, et al. Adult-onset painful axonal polyneuropathy caused by a dominant NAGLU mutation. Brain 2015;138:1477–1483.